

This is the peer reviewed version of the following article:

Computational evidence support the hypothesis of neuroglobin also acting as an electron transfer species / Paltrinieri, Licia; Di Rocco, Giulia; Battistuzzi, Gianantonio; Borsari, Marco; Sola, Marco; Ranieri, Antonio; Zanetti Polzi, Laura; Daidone, Isabella; Bortolotti, Carlo Augusto. - In: JBIC. - ISSN 0949-8257. - 22:4(2017), pp. 615-623. [10.1007/s00775-017-1455-2]

Terms of use:

The terms and conditions for the reuse of this version of the manuscript are specified in the publishing policy. For all terms of use and more information see the publisher's website.

18/12/2025 11:08

Computational evidences support the hypothesis of neuroglobin also acting as an electron transfer species

Licia Paltrinieri,¹ Giulia Di Rocco,¹ Gianantonio Battistuzzi,² Marco Borsari,² Marco Sola,¹
Antonio Ranieri,¹ Laura Zanetti-Polzi,³ Isabella Daidone,³✉ Carlo Augusto Bortolotti,^{1,4}✉

¹ Department of Life Sciences, University of Modena and Reggio Emilia, Via Campi 103, 41125, Modena, Italy

² Department of Chemical and Geological Sciences, University of Modena and Reggio Emilia, Via Campi 103, 41125, Modena, Italy

³ Department of Physical and Chemical Sciences, University of L'Aquila, via Vetoio (Coppito 1), 67010 L'Aquila (Italy)

⁴ Center S3, CNR NANO, Institute of Nanoscience, Via Campi 213/A, 41125, Modena, Italy

✉ Send correspondence to:

carloaugusto.bortolotti@unimore.it, tel: +39 059 2058608, fax: +39 0592055131

isabella.daidone@univaq.it, tel: +39 0862433754, fax: +39 0862433753

Keywords: hexa-coordinated globins, reorganization energy, Perturbed Matrix Method, molecular dynamics, cytochrome *c*, reduction potential, thermodynamics

Abstract

Neuroglobin (Ngb) is a recently identified hexa-coordinated globin, expressed in the nervous system of humans. Its physiological role is still debated: one hypothesis is that Ngb serves as an electron transfer (ET) species, possibly by reducing cytochrome *c* and preventing it to initiate the apoptotic cascade. Here, we use the Perturbed Matrix Method (PMM), a mixed quantum mechanics/molecular dynamics approach, to investigate the redox thermodynamics of two neuroglobins, namely the human Ngb and GLB-6 from invertebrate *Caenorhabditis elegans*. In particular, we calculate the reduction potential of the two globins, resulting in an excellent agreement with the experimental values, and we predict the reorganization energies, λ , which have not been determined experimentally yet. The calculated λ values match well those reported for

known ET proteins and thereby support a potential involvement *in vivo* of the two globins in ET processes.

Introduction

The investigation of the thermodynamics and kinetics of electron transfer (ET) processes in biology is crucial to both a thorough understanding of the role played by a protein *in vivo* [1, 2], but also to facilitate the design of constantly increasing bio-inspired applications in fields like artificial photosynthesis, biofuel cells or bioelectronics [3–5] .

Electrochemistry and spectroscopy are among the experimental methods of choice for monitoring changes in ET efficiency of a protein under different environmental conditions. Nevertheless, these methods, despite being highly informative on the functional properties of the investigated species, cannot provide a direct link between activity and structure with atomistic detail. Yet, it is becoming now widely accepted that the functionality of a biomolecule is ultimately defined not strictly by its structure but rather by how the latter changes along time, i.e. by its dynamics [6, 7]. Therefore, the possibility to combine functional investigations with time-dependent information at the atomic/molecular level represents an ideal strategy to disentangle the complex dynamics/function relationship in biological systems.

Experimental techniques to sample protein dynamics still suffer of insufficient spatial or temporal resolution [8]; a solid alternative is represented by computational methods, that can provide an extensive conformational sampling coupled to atomistic spatial resolution.

Among computational methods to investigate ET reactions [1, 9–11] a recently developed hybrid method based on molecular dynamics (MD) simulations and the Perturbed Matrix Method (PMM), the MD-PMM approach, has been successfully employed to elucidate the redox properties of different ET species proteins: *c*-type cytochromes (both in solution and immobilised on a surface), blue copper proteins and multiheme cytochromes *c* [12–16].

In this paper, the focus is on a different family of proteins, called globins. Globins are relatively small heme proteins, characterised by a common fold formed by 5 to 8 α -helices and containing a single heme *b* [17, 18]. The two most representative members of the globins family, Myoglobin (Mb) and Hemoglobin (Hb), feature a pentacoordinate heme iron, and the sixth, vacant position can reversibly bind an exogenous ligand: Mb and Hb use it for the transport and storage of O₂. About fifteen years ago, new globin proteins, different from the known Hb and Mb were discovered and found to be present in very diverse organisms [19, 20], from vertebrate to plants and bacteria.

Among these new proteins, of particular interest is a class of globins containing a six-coordinate heme group [19, 21]. Neuroglobin (Ngb), which is mostly localized in the nervous tissues [19, 22], is one of the most interesting members of this class. Ngb has been gaining increasing attention in the last ten years, but its physiological role is far from being unambiguously understood. Various functions for this protein have been proposed so far [23–25]: some studies assign to Ngb a myoglobin-like role, suggesting that it could act to supply O₂ to the nervous cells, where Mb is not present, protecting them in case of hypoxia and ischemia [18, 26]. Other potential physiological roles suggested for Ngb include the tuning of NO regulation in tissues [25], by detoxification of damaging surplus of NO to NO₃[−] or, conversely, by the production of NO from NO₂[−] for signalling functions [27–29]. Moreover, Ngb may be involved in scavenging dangerous reactive oxygen or nitrogen species (ROS and RNS, respectively) [30], or can participate to redox processes, interacting with cytochrome *c* (cyt *c*) to limit apoptosis in cytosol [31–33]. The latter proposed function is one of the most intriguing, and it is supported by the experimental evidence that ferrous Ngb can reduce ferric cyt *c*, which is involved in the apoptotic process, while the ferrous cyt *c* is apparently inactive in the initiation of apoptosis [34].

In this paper, we apply the MD-PMM approach to investigate the redox properties of two members of the neuroglobin family, namely human Ngb and a neural globin (GLB-6) from the nematode *Caenorhabditis elegans*. The latter was chosen because it poses interesting questions to the study of the structure/function relationship in globins, thanks to its peculiar properties in terms of affinity

towards exogenous ligands and redox reactivity [35]. In fact, unlike other hexa-coordinated globins, GLB-6 does not bind NO, CN⁻ nor CO, and is rapidly oxidized by O₂. Our goal is to gain new insights into the possible physiological role(s) played by Ngb in vivo, by using a PMM-based approach to the investigation of biomolecules featuring a Bis-His iron ligation, which is rather common in ET metalloproteins [36].

Theory and Methods

Quantum chemical calculations

A QC to be explicitly treated at the electronic level is necessary for the MD-PMM procedure to be applied (see above). In the present case, the atoms of the prosthetic group and of the side chains of the axial ligands, i.e., the side chains of the two histidines, were selected as QC. Quantum chemical calculations were previously performed on the isolated QC for both redox states (i.e., with Fe⁺² and Fe⁺³) [14] and are here briefly summarized. To obtain the unperturbed ground-state geometry, energy, and related properties of the QC for both of its redox states quantum chemical calculations were performed on the isolated QC at the time dependent density functional theory (TD-DFT) level with Becke's three-parameter exchange and Lee, Yang, and Parr correlation functionals (B3LYP). The atomic basis sets were as follows: (i) for the iron atom, we used the LANL2DZ effective core potential for the inner electrons and a double Gaussian basis set of (5S,5P,5D)/[3S,3P,2D] quality for the valence electrons [37]; (ii) for the hydrogen, carbon, nitrogen, and oxygen atoms, we used a standard 6-31+G(d) [38] Gaussian basis set. The first 12 unperturbed excited electronic (vertical) states were obtained on the ground state geometry using TD-DFT calculations for both redox states. Although in general this level of theory might not provide a fully correct description of electronic excited states, in the case of the heme group, it has already proved to represent a good compromise between computational costs and chemical accuracy [12]. All quantum chemical calculations were carried out using the Gaussian 03 package (see also Electronic Supplementary Material).

The Perturbed Matrix Method

In MD-PMM calculations, similarly to quantum mechanics/molecular mechanics (QM/MM) procedures [9, 39], a portion of the system to be treated at electronic level is pre-defined (the quantum centre, QC), with the rest of the system described at a classical atomistic level exerting an electrostatic effect on the QC. With a relatively low computational cost, the MD-PMM can be applied to a very large set of molecular configurations, hence providing the dynamical coupling of electronic properties with classical degrees of freedom. Indeed, the phase space sampling is provided by classical molecular dynamics and thus a statistically relevant sampling of the QC/environment configurations can be achieved, which is necessary for a proper description of functional properties in dynamical, complex systems.

At variance with other QM/MM approaches, here the effect of the environment is not obtained by selecting a limited number of snapshots from the MD sampling, but rather by calculating, for each configuration generated by the explicit solvent MD simulation, the electrostatic effect of the instantaneous atomistic configurations of the environment as perturbing term to the electronic properties of the isolated QC. Therefore, one first evaluates an orthonormal set of unperturbed (i.e., isolated *in vacuo*) electronic Hamiltonian eigenfunctions on the QC of interest, and then calculates the perturbed Hamiltonian matrix, whose diagonalization leads to perturbed electronic energies. If the considered QC is rigid (or quasi-rigid), as in the present case, the quantum calculations are performed only once on the optimized geometry of the QC in vacuum. If the QC is not rigid, a number of quantum calculations are performed on the relevant conformations of the QC.

More details on this method can be found in Electronic Supplementary Materials and in previous works [12, 13, 15, 16, 40, 41].

For the more specific task of calculating E^0 in redox-active proteins, the perturbed electronic ground-state energies are calculated for the QC reduced and oxidised chemical states, providing the perturbed electronic ground-state energy shift. Also, the perturbing environment configurations are obtained by classical MD simulations performed in both the reduced and oxidised ensemble, i.e.

with the QC in the reduced and oxidised chemical state, respectively. The (Helmholtz) free energy change ΔA^0 upon reduction (related to the redox potential E^0 via $E^0 = -\Delta A^0/F$, with F the Faraday constant) can be calculated using the following equation [42]:

$$\beta(\Delta A^0) = -\ln \frac{\langle e^{-\frac{\beta \Delta \mathcal{U}}{2}} \rangle_{ox}}{\langle e^{+\frac{\beta \Delta \mathcal{U}}{2}} \rangle_{red}} \quad (1)$$

In the above equation, $\Delta \mathcal{U}$ is the electron transfer transition energy $\Delta \mathcal{U} = \mathcal{U}_{red} - \mathcal{U}_{ox}$, where \mathcal{U}_{red} and \mathcal{U}_{ox} are the perturbed electronic ground-state energies of the quantum centre for the reduced and oxidized state, respectively [12–14] and $\beta = 1/kT$. The associated standard error for the calculated E^0 is 0.015 V, obtained by averaging the estimated standard errors of the reduction potentials for all the investigated reduction processes.

To achieve a more solid estimate of the reduction free energy, the values calculated by using Eq. 1 were also compared with the ones obtained by using other free energy estimation methods: the arithmetic average (AA) of the values obtained in the reduced and oxidized ensemble [12], the Bennet's method [43] and the Third Power Fitting (TPF) thermodynamic integration [44, 45]. More details on these methods can be found in the Electronic Supplementary Materials.

For the calculation of reorganization energies, we followed our recently published procedure [14, 46] to calculate λ as the average of λ_{red} and λ_{ox} , corresponding to the relaxation free energy for the oxidized to reduced or reduced to oxidized state transitions, respectively. The two distinct reorganization free energies can be calculated as [46]:

$$\lambda_{red} = \langle \Delta \mathcal{U} \rangle_{ox} - \Delta A^0 - kT \ln \frac{\sigma_{red}}{\sigma_{ox}} \quad (2)$$

$$\lambda_{ox} = -\langle \Delta \mathcal{U} \rangle_{red} + \Delta A^0 + kT \ln \frac{\sigma_{red}}{\sigma_{ox}} \quad (3)$$

with σ_{red} and σ_{ox} the standard deviations of the corresponding transition energy distributions. λ_{red} and λ_{ox} are then used to calculate the mean values $\lambda = (\lambda_{red} + \lambda_{ox}) / 2$ for both species.

Molecular dynamics simulations

The crystal structure of human neuroglobin (PDB ID code: 4MPM [47], chain B) and GLB-6 from *C. elegans* (PDB ID code: 3MVC [35], chain A) were used as the starting point for the MD simulations. The crystal structure of human neuroglobin lacks the first and the last two residues, while the crystal structure of GLB-6 lacks residues from 124 to 127. Both proteins are then modelled using the EasyModeller software (version 4.0) [48], using as input the corresponding FASTA sequence and as template the corresponding PDB structure, in order to obtain the two complete proteins. The GROMACS software package [49], version 4.5.5, was used for all the MD simulations. The proteins were put at the centre of a 109 nm^3 dodecahedral box filled with single point charge (SPC) water molecules [50] at the typical liquid water density (55.32 mol/l) and six Na^+ ions for neuroglobin and three Cl^- ions for GLB-6. The volume of the simulation box was chosen in order to achieve a distance between the QC and the wall of the box of $\approx 3 \text{ nm}$, large enough in order to avoid artifacts resulting from computing the free-energy difference of a full charge change, from a finite system [51]. A test previously performed on a similar system showed that such a distance assures the independence of the calculated reduction potential upon the dimensions of the box [15]: in that case a test simulation with a bigger box showed that the calculated perturbed ground state energies are not affected by the dimension of the box. The parameters for the proteins and the hemes in their reduced form were taken from the Gromos96 (53a6 version) force field, whereas the atomic partial charges and the missing parameters for the heme group and its axial ligands in their oxidised form were taken from ref. [12]. For all the simulations, a standard protocol was used: firstly, the systems energy was minimised in vacuum, using the steepest descent method; then, after the addition of the solvent and counter-ions, a two-step minimisation protocol was performed with the conjugate gradient method. The first minimisation held fixed the coordinates of the proteins, allowing only the water and counter-ions to move. The second minimisation involves both the protein and solvent molecules. Then the temperature of the systems was gradually increased from 50 to 300 K in a 100 ps MD run, and was kept constant for all the simulation time by the isokinetic temperature coupling [52]. The simulation

runs were performed in the NVT ensemble. The bond lengths were constrained with the LINCS algorithm [53] and an integration step of 2.0 fs was used for the integration of the equation of motion. The Particle Mesh Ewald (PME) method [54] was used to compute the long-range electrostatics, with a grid spacing of 0.12 nm, a fourth-order cubic interpolation and a real space cut-off of 0.9 nm.

Results and discussion

Despite a rather low sequence identity (less than 30%), the structure of Ngb closely resembles that of a typical Mb [18]. Ngb is a monomer of about 150 residues, depending on the species, with a molecular mass of 17 kDa [19]. It features the typical globin fold [19, 20], with 8 α -helices arranged in a "three-over-three" α -helical sandwich [17, 18] (see Fig.1a, left panel). The three-dimensional structure of GLB-6 is very similar to that of Ngb (see Fig.1a, right panel), with seven helices arranged in the typical globin fold and featuring a heme iron axially coordinated by two His residues.

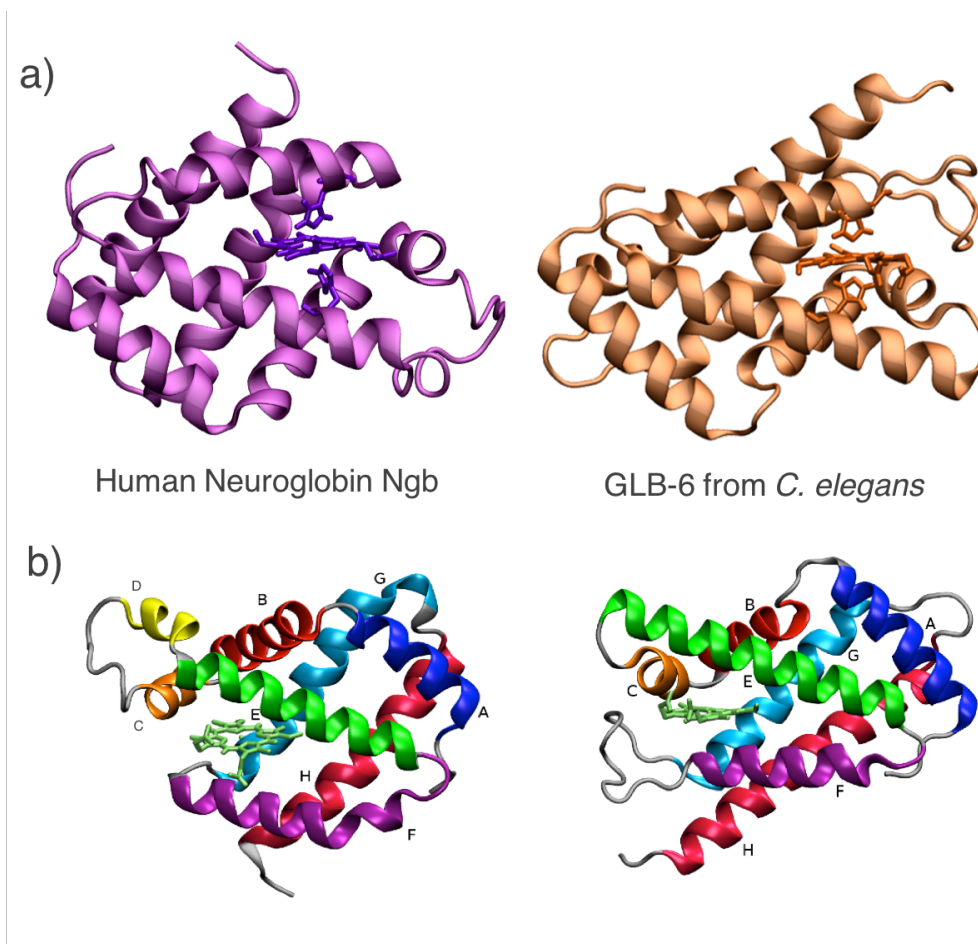


Figure 1. a) Cartoon representation of the three-dimensional structure of human neuroglobin, PDB ID code: 4MPM [47], (left) and of GLB-6 from *C. elegans*, PDB ID code: 3MVC [35]. The heme site is represented as licorice. b) Cartoon representation of both proteins, rotated with respect to top view, with α -helices in different colours and labelled A to H. Please note that the short D helix is missing in GLB-6. The image was prepared using the VMD software [55].

The calculation of the reduction potential E^0 for Ngb and GLB-6 was performed using the MD-PMM approach, following the same strategy that had been successfully employed to investigate the redox thermodynamics of other ET proteins. We first performed 100 ns-long molecular dynamics (MD) simulations of both globins at infinite dilution in both their reduced and oxidized ensemble. We then applied the PMM approach to evaluate the (Helmholtz) free-energy change upon reduction, using equation 1.

The calculated E^0 values are reported in Table 1, where they are compared to the corresponding experimental values. Moreover, we benchmarked our approach against other theoretical methods for the calculation of reduction free energy: two of them are based on Free Energy Perturbation (FEP), and they involve Bennet's method [43] and the arithmetic average (AA) of the values obtained in the reduced and oxidized ensemble [12], respectively. The third method is the Third Power Fitting (TPF) thermodynamic integration [44].

	E^0_{calc} (Lu)	$E^0_{\text{exp}}^b$	E^0_{calc} (Bennet)	E^0_{calc} (AA)	E^0_{calc} (TPF)
GLB-6	4.148	4.227	4.080	4.132	4.108
Ngb	4.241	4.305	4.192	4.236	4.201

Table 1. Comparison between calculated and experimental E^0 values. All values are expressed in Volts. ^b Experimental values are taken from ref. [35]

Please note that, in order to allow for a direct comparison, absolute experimental values were obtained by adding the IUPAC recommended 4.420 V value for the hydrogen semi-reaction to the E^0 vs. SHE [56]. All estimates provided by the tested computational approaches are within 7 kJ/mol (approximately 70 mV). In particular, the Lu and AA methods give very similar estimates with a smaller difference from the experimental values with respect to the Bennet and TPF methods. Since the Lu approach yields the calculated E^0 closest to experimental values we consider it the best choice for calculating the reduction free energy (see the Electronic Supplementary Materials for more details).

The comparison shows a very good agreement between the calculated and experimental values, with $E^0_{\text{calc}} - E^0_{\text{exp}}$ being 89 mV and 64 mV for GLB-6 and Ngb, respectively. This difference is $\approx 2\%$ of the absolute redox potential for both proteins, is likely to mostly depend on the level of the quantum chemical calculations of the QC and on the approximations of the classical force field used. Moreover, since the PMM method is based on first-principles and does not involve fitting to experiment, it may not always reproduce the exact absolute experimental values. Most importantly,.

our calculations reproduce very well the difference, both in terms of sign and magnitude, between the reduction potential for the two species, within the associated error: the observed ΔE^0_{exp} is 78 mV, and $\Delta E^0_{\text{calc}} = 93$ mV. This is also due to the fact that the ΔE^0_{calc} is independent of the choice of the value for the hydrogen semi-reaction. The more negative reduction potential of GLB-6 might be explained based on comparison of its tertiary structure with that of Ngb. The F helix is shorter in GLB-6 than in Ngb, and GLB-6 also features a longer F-G loop. As a consequence, in GLB-6 the proximal iron axial ligand His92, located at the end of the F helix, is more exposed to the solvent than in Ngb, resulting in the ferric state being thermodynamically favoured over the reduced ferrous one [57].

The good agreement between theoretical and experimental reduction potentials proves the reliability of the MD-PMM approach in the investigation of the redox thermodynamic properties of hexa-coordinated globins. Therefore, we could further proceed in using our sampling to predict other physical quantities, which have not been determined experimentally yet.

We hence used the MD-PMM approach to calculate the reorganization free energy λ , a crucial quantity in the description of ET processes: λ can be defined as the energy needed for the reactants to move from the equilibrium reactant geometry to the equilibrium product geometry, without transferring electrons [58].

It is worth highlighting that the experimental determination of reorganization energy is far from straightforward, and the reliability of some of the most widely used approaches to obtain λ (e.g. measuring the temperature dependence of ET rate constants and fitting to the Marcus classical equation) is debated [59]. Moreover, reported λ values for the same species may differ significantly, depending on the experimental conditions under which the reorganization free energy were obtained; for surface-immobilised proteins, for example, λ values might lack the entropic contribution of the solvent reorganization [60], which is instead significant in experiments performed for freely diffusing species [2, 61], and therefore *in vivo*. In general, electrochemical

measurements at varying temperatures yield the direct determination of the activation enthalpy ΔH^\ddagger , which is equivalent to an activation free energy ΔG^\ddagger (the thermodynamic quantity directly related to λ via $\Delta G^\ddagger = (\Delta G^0 + \lambda)^2 / 4\lambda$) only under the assumption that $\Delta S^\ddagger = 0$, which is not always valid [62, 63]. Therefore, a theoretical approach allowing for the calculation of λ represents an invaluable tool in the framework of the elucidation of biological ET, also offering the possibility to relate this observable to the structure and dynamics of the biomolecule.

The reorganization energies λ_{red} and λ_{ox} calculated with equations 2 and 3 for both Ngb and GLB-6 are shown in Table 2, together with their mean value λ .

	λ_{red} (eV)	λ_{ox} (eV)	λ (eV)
GLB-6	0.84	1.01	0.92
Ngb	0.62	0.80	0.71

Table 2. Reorganization energies obtained with the MD-PMM method for the two investigated systems. The standard errors for λ are 0.02 eV, obtained by averaging the associated standard errors from all the simulations.

The estimated λ values for both globins lie in the range of the typical calculated λ values for electron transfer proteins. The reported reorganization free energy for biological systems approximately span 1 eV, ranging from very low λ (approx. 0.25-0.5 eV) for deeply buried redox couples in the bacterial reaction centre [64] to λ as large as 1.5 eV for redox couples with at least one partner fully exposed to solvent [65]. The majority of reorganization energy for tunnelling within ET proteins typically range between 0.6 and 0.9 eV, when the redox cofactors are shielded from direct contact with water or only partly solvent exposed. This is the case of the two paradigmatic ET proteins cyt *c* (for which reorganization free energy values ranging from 0.5 to 1.5 eV have been reported [58, 66, 67]) and azurin (0.6 to 0.8 eV [61, 68]).

The molecular determinants to the predicted λ values might be sought in the analysis of the structural and dynamical features of the systems sampled with the MD simulations, and in particular on how the dynamics of the reduced form of each globin differs from that of its oxidized counterpart. Fig. 2 shows the comparison of the Root Mean Square Fluctuation (RMSF) per C α atom in the reduced and oxidized species: for both Ngb and GLB-6, the RMSF profiles for the two redox states are almost superimposable, suggesting that the flexibility is not significantly affected by the redox state of the active site.

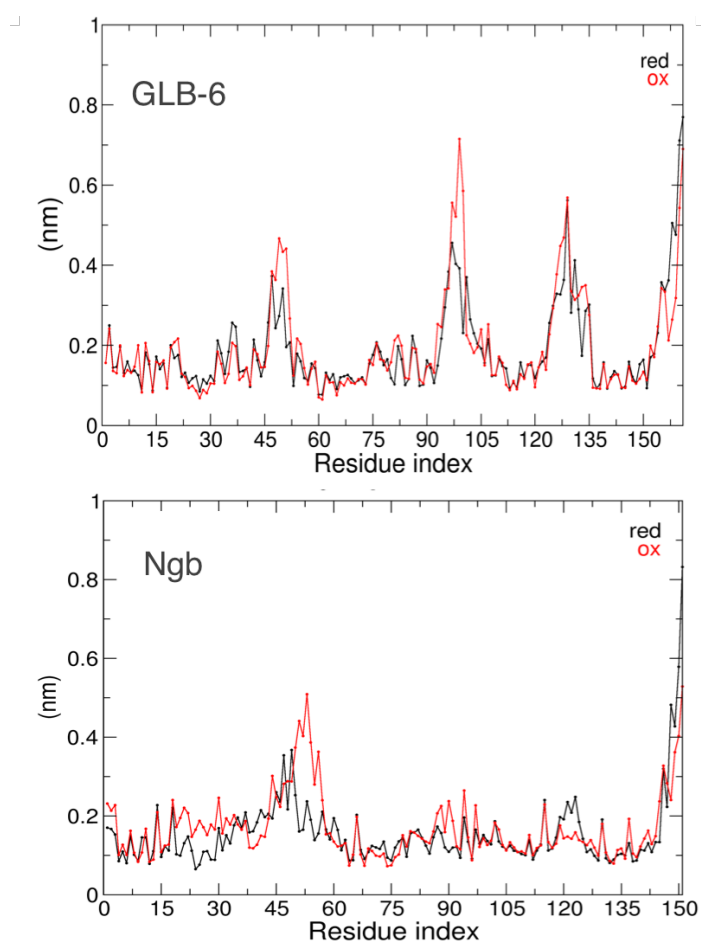


Figure 2. Calculated RMSF for a) GLB-6 from *C. elegans* and b) Ngb, respectively, in both reduced (black) and oxidized (red) ensembles.

The Essential Dynamics analysis [69] on the C α atoms was used as a tool to further analyse, and visualize, the fluctuations in the simulations. The trace of the covariance matrix, which accounts for the overall amount of motion, is similar for the reduced and oxidized protein for both Ngb and GLB-6 (the difference between the trace of the covariance matrix for the reduced and oxidized protein is lower than 0.1 nm²). Moreover, for both Ngb and GLB-6 the essential subspace spanned by the first three eigenvectors, and describing 50% of the total fluctuations, is similar in the oxidized and reduced state. As an example, in Fig. 3, the eigenvalues of the first 40 eigenvectors for Ngb in the reduced and oxidized states are displayed, together with, the superimposition of 10 configurations obtained projecting the C α motion along the first eigenvector. In Fig. S1, the first eigenvector components per residue are displayed in both oxidation states. It is apparent that, for both species, the dominant motions are very similar in the two redox states, with approximately the same residues contributing to the highest amplitude motion.

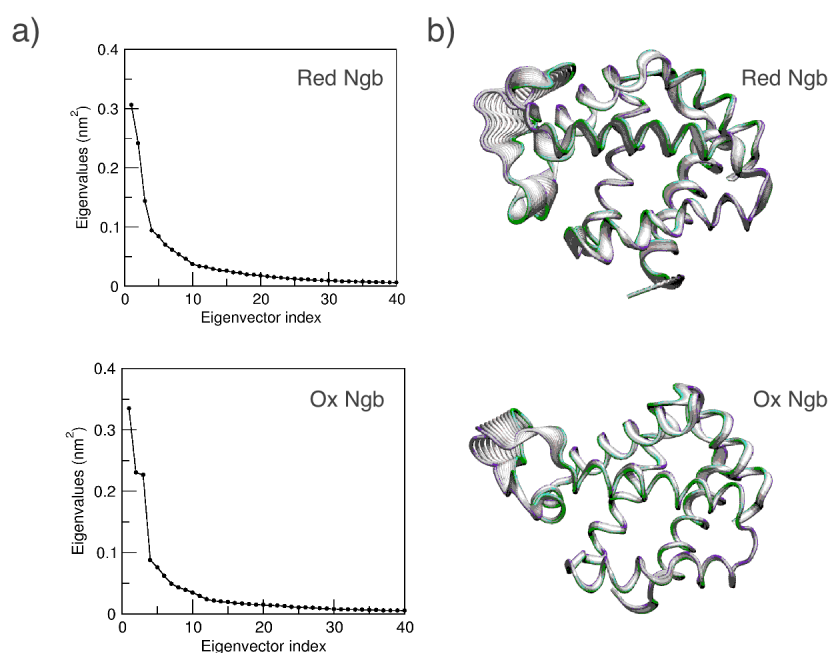


Figure 3. a) Eigenvalues of the first 40 eigenvectors for reduced (top) and oxidized (bottom) Ngb. b) Superimposition of 10 configurations obtained projecting the C α motion along the first eigenvector for reduced (top) and oxidized (bottom) Ngb.

The estimated λ values are in line with those of widely investigated redox metalloproteins, and in qualitative agreement with the experimental values trend of rates of ET processes between different globins and cyt *c* [70]. Spectroscopic investigations [70] show that human Ngb and GLB-26 from *C. elegans* display ET rate values that are three to four orders of magnitude higher than those exhibited by another hexa-coordinated globin, cytoglobin (Cygb) and horse myoglobin, respectively. GLB-26 is analogous to GLB-6, especially in terms of inability to bind O₂ reversibly [70]; for both GLB-26 and Ngb, an electron transfer role physiological has been suggested, while such hypothesis was never put forward for Cygb. The strong hexacoordination featured by Ngb and GLB-26 most likely lowers the reorganization energy for these two species, resulting in higher values of ET rates to cyt *c*. The presence of a bis-histidyl, tightly six-coordinated heme iron for both ferric and ferrous states is known to impact significantly on the rate of reduction of globins, most likely by lowering the degree of heme-pocket reorganization upon switching between Fe³⁺ and Fe²⁺, at variance with most pentacoordinate globins [71, 72] that feature a water molecule as sixth axial ligand in the ferric state.

Our findings therefore seem to back up the hypothesis that hexa-coordinated globin might fulfil ET roles *in vivo*. In particular, as anticipated in the Introduction, Ngb was assigned a role as potential reducing agent for cyt *c*. This possible pathway is supported by the sign and magnitude of the difference between the reduction potential of the two species (with cyt *c* featuring a more positive E^0 than Ngb), by the experimentally determined electron transfer rate constant of the ET process between Ngb and cyt *c* is equal to $2.0 \times 10^7 \text{ M}^{-1} \text{ s}^{-1}$ [31] (a value very close to the one of the reaction between cyt *c* and cyt *c* oxidase [73]) and eventually by the putative structures of the Ngb/cyt *c* predicted computationally [32, 74] .

Conclusions

Based on the combined use of the classical sampling provided by the MD and the calculation of electronic properties via the PMM, we have been able to reliably predict the hexa-coordinated free

energy for the two globins Ngb and GLB-6. The estimated values are reasonably low and fall within the range of λ for electron transfer proteins; they can be ascribed to minimal structural rearrangements and only minor differences in the dynamic signature between the reduced and oxidized form. The findings support the hypothesis of neuroglobin featuring, among others, a potential role as an electron transfer species. Our results contribute to portraying hexa-coordinated globins as versatile proteins, fulfilling different tasks, according to cellular compartmentalisation and environmental changes [70]. The idea of hexacoordinated globins potentially fulfilling different functions has been already hypothesized [21, 70, 75]: in the case of Ngb, multiple functionality might be provided by its displaceable hexacoordination [21], which would not be necessary if Ngb was meant to work solely as ligand transporter or purely ET species. Future experiments will tell whether human Ngb can be considered as a moonlighting protein, i.e. a multifunctional biomolecule performing distinct physiological functions using the same protein domain [76, 77], in response to changes in cell type and localization or concentration of biomolecules such as ligands or cofactors.

Acknowledgements

We acknowledge the CINECA award under the ISCRA initiative for the availability of high performance computing resources and support. We thank Andrea Amadei and Massimiliano Aschi for fruitful discussions.

Supplementary Material:

Details on the quantum chemical calculations and on the theoretical methods for the estimation of the reduction potential; First eigenvector components for GLB-6 and Ngb.

References

1. Blumberger J (2015) Recent Advances in the Theory and Molecular Simulation of Biological Electron Transfer Reactions. *Chem Rev* 115:11191–11238. doi:

10.1021/acs.chemrev.5b00298

2. Gray HB, Winkler JR (2003) Electron tunneling through proteins. *Q Rev Biophys* 36:341–372. doi: 10.1017/S0033583503003913
3. Fukuzumi S (2008) Development of bioinspired artificial photosynthetic systems. *Phys Chem Chem Phys* 10:2283–2297. doi: 10.1039/B801198M
4. Minteer SD, Liaw BY, Cooney MJ (2007) Enzyme-based biofuel cells. *Curr Opin Biotechnol* 18:228–234. doi: <http://dx.doi.org/10.1016/j.copbio.2007.03.007>
5. Lovley DR (2012) Electromicrobiology. *Annu Rev Microbiol* 66:391–409. doi: 10.1146/annurev-micro-092611-150104
6. Henzler-Wildman K, Kern D (2007) Dynamic personalities of proteins. *Nature* 450:964–72. doi: 10.1038/nature06522
7. Frauenfelder H, Chen G, Berendzen J, et al (2009) A unified model of protein dynamics. *Proc Natl Acad Sci* 106:5129–5134. doi: 10.1073/pnas.0900336106
8. Sagle LB, Zimmermann J, Matsuda S, et al (2006) Redox-coupled dynamics and folding in cytochrome c. *J Am Chem Soc* 128:7909–15. doi: 10.1021/ja060851s
9. Sigfridsson E, Olsson MHM, Ryde U (2001) Inner-sphere reorganization energy of iron-sulfur clusters studied with theoretical methods. *Inorg Chem* 40:2509–2519. doi: 10.1021/ic000752u
10. Simonson T (2002) Gaussian fluctuations and linear response in an electron transfer protein. *Proc Natl Acad Sci U S A* 99:6544–9. doi: 10.1073/pnas.082657099
11. Migliore A, Corni S, Di Felice R, Molinari E (2006) First-principles density-functional theory calculations of electron-transfer rates in azurin dimers. *J Chem Phys* 124:64501. doi: 10.1063/1.2166233
12. Bortolotti CA, Amadei A, Aschi M, et al (2012) The reversible opening of water channels in cytochrome c modulates the heme iron reduction potential. *J Am Chem Soc* 134:13670–8. doi: 10.1021/ja3030356

13. Daidone I, Amadei A, Zaccanti F, et al (2014) How the Reorganization Free Energy Affects the Reduction Potential of Structurally Homologous Cytochromes. *J Phys Chem Lett* 5:1534–1540.
14. Daidone I, Paltrinieri L, Amadei A, et al (2014) Unambiguous Assignment of Reduction Potentials in Diheme Cytochromes. *J Phys Chem B* 118:7554–7560. doi: 10.1021/jp506017a
15. Zanetti-Polzi L, Daidone I, Bortolotti CA, Corni S (2014) Surface packing determines the redox potential shift of cytochrome c adsorbed on gold. *J Am Chem Soc* 136:12929–37. doi: 10.1021/ja505251a
16. Zanetti-Polzi L, Bortolotti CA, Daidone I, et al (2015) A few key residues determine the high redox potential shift in azurin mutants. *Org Biomol Chem* 13:11003–11013. doi: 10.1039/C5OB01819F
17. Holm L, Sander C (1993) Structural alignment of globins, phycocyanins and colicin A. *FEBS Lett* 315:301–306. doi: 10.1016/0014-5793(93)81183-Z
18. Pesce A, Dewilde S, Nardini M, et al (2003) Human brain neuroglobin structure reveals a distinct mode of controlling oxygen affinity. *Structure* 11:1087–1095. doi: 10.1016/S0969-2126(03)00166-7
19. Burmester T, Weich B, Reinhardt S, Hankeln T (2000) A vertebrate globin expressed in the brain. *Nature* 407:520–523. doi: 10.1038/35035093
20. Trent JT, Watts RA, Hargrove MS (2001) Human Neuroglobin, a Hexacoordinate Hemoglobin That Reversibly Binds Oxygen. *J Biol Chem* 276:30106–30110. doi: 10.1074/jbc.C100300200
21. Halder P, Trent III J, Hargrove M (2007) Influence of the Protein Matrix on Intramolecular Histidine Ligation in Ferric and Ferrous Hexacoordinate Hemoglobins. *Proteins* 66:172–182. doi: 10.1002/prot
22. Dewilde S, Kiger L, Burmester T, et al (2001) Biochemical Characterization and Ligand Binding Properties of Neuroglobin, a Novel Member of the Globin Family. *J Biol Chem*

276:38949–38955. doi: 10.1074/jbc.M106438200

23. Burmester T, Hankeln T (2009) What is the function of neuroglobin? *J Exp Biol* 212:1423–1428. doi: 10.1242/jeb.000729
24. Ascenzi P, Gustincich S, Marino M (2014) Mammalian nerve globins in search of functions. *IUBMB Life* 66:268–276. doi: 10.1002/iub.1267
25. Burmester T, Hankeln T (2014) Function and evolution of vertebrate globins. *Acta Physiol* 211:501–514. doi: 10.1111/apha.12312
26. Pesce A, Bolognesi M, Bocedi A, et al (2002) Neuroglobin and cytoglobin. Fresh blood for the vertebrate globin family. *EMBO Rep* 3:1146–1151. doi: 10.1093/embo-reports/kvf248
27. Brunori M, Giuffrè A, Nienhaus K, et al (2005) Neuroglobin, nitric oxide, and oxygen: functional pathways and conformational changes. *Proc Natl Acad Sci U S A* 102:8483–8. doi: 10.1073/pnas.0408766102
28. Giuffrè A, Moschetti T, Vallone B, Brunori M (2008) Is neuroglobin a signal transducer? *IUBMB Life* 60:410–413. doi: 10.1002/iub.88
29. Tiso M, Tejero J, Basu S, et al (2011) Human neuroglobin functions as a redox-regulated nitrite reductase. *J Biol Chem* 286:18277–18289. doi: 10.1074/jbc.M110.159541
30. Fago A, Hundahl C, Dewilde S, et al (2004) Allosteric regulation and temperature dependence of oxygen binding in human neuroglobin and cytoglobin: Molecular mechanisms and physiological significance. *J Biol Chem* 279:44417–44426. doi: 10.1074/jbc.M407126200
31. Fago A, Mathews AJ, Moens L, et al (2006) The reaction of neuroglobin with potential redox protein partners cytochrome b5 and cytochrome c. *FEBS Lett* 580:4884–4888. doi: 10.1016/j.febslet.2006.08.003
32. Bønding SH, Henty K, Dingley AJ, Brittain T (2008) The binding of cytochrome c to neuroglobin: A docking and surface plasmon resonance study. *Int J Biol Macromol* 43:295–299. doi: 10.1016/j.ijbiomac.2008.07.003

33. Brittain T, Skommer J (2012) Does a redox cycle provide a mechanism for setting the capacity of neuroglobin to protect cells from apoptosis? *IUBMB Life* 64:419–422. doi: 10.1002/iub.566
34. Suto D, Sato K, Ohba Y, et al (2005) Suppression of the pro-apoptotic function of cytochrome c by singlet oxygen via a haem redox state-independent mechanism. *Biochem J* 392:399–406. doi: 10.1042/BJ20050580
35. Yoon J, Herzik MA, Winter MB, et al (2010) Structure and properties of a bis-histidyl ligated globin from *Caenorhabditis elegans*. *Biochemistry* 49:5662–5670. doi: 10.1021/bi100710a
36. Liu J, Chakraborty S, Hosseinzadeh P, et al (2014) Metalloproteins containing cytochrome, iron-sulfur, or copper redox centers. *Chem Rev* 114:4366–469. doi: 10.1021/cr400479b
37. Hay PJ, Wadt WR (1985) Ab initio effective core potentials for molecular calculations. Potentials for K to Au including the outermost core orbitals. *J Chem Phys* 82:299.
38. Krishnan R, Binkley JS, Seeger R, Pople JA (1980) Self-consistent molecular orbital methods. XX. A basis set for correlated wave functions. *J Chem Phys* 72:650–654.
39. Blumberger J (2008) Free energies for biological electron transfer from QM/MM calculation: method, application and critical assessment. *Phys Chem Chem Phys* 10:5651–67. doi: 10.1039/b807444e
40. Zanetti Polzi L, Amadei A, Aschi M, Daidone I (2011) New Insight into the IR-Spectra/Structure Relationship in Amyloid Fibrils: A Theoretical Study on a Prion Peptide. *J Am Chem Soc* 133:11414–11417.
41. Zanetti-Polzi L, Aschi M, Amadei A, Daidone I (2013) Simulation of the Amide I Infrared Spectrum in Photoinduced Peptide Folding/Unfolding Transitions. *J Phys Chem B* 117:12383–12390.
42. Lu N, Singh JK, Kofke DA (2003) Appropriate methods to combine forward and reverse free-energy perturbation averages. *J Chem Phys* 118:2977–2984. doi: 10.1063/1.1537241

43. Bennett CH (1976) Efficient estimation of free energy differences from Monte Carlo data. *J Comput Phys* 22:245–268. doi: [http://dx.doi.org/10.1016/0021-9991\(76\)90078-4](http://dx.doi.org/10.1016/0021-9991(76)90078-4)
44. de Ruiter A, Oostenbrink C (2012) Efficient and Accurate Free Energy Calculations on Trypsin Inhibitors. *J Chem Theory Comput* 8:3686–3695. doi: 10.1021/ct200750p
45. Chipot C, Pohorille A (2007) Free Energy Calculations - Theory and Applications in Chemistry and Biology. doi: 10.1007/978-3-540-38448-9
46. Amadei A, Daidone I, Bortolotti CA (2013) A general statistical mechanical approach for modeling redox thermodynamics: the reaction and reorganization free energies. *RSC Adv* 3:19657. doi: 10.1039/c3ra42842g
47. Guimarees BG, Hamdane D, Lechauve C, et al (2014) The crystal structure of wild-type human brain neuroglobin reveals flexibility of the disulfide bond that regulates oxygen affinity. *Acta Crystallogr Sect D Biol Crystallogr* 70:1005–1014. doi: 10.1107/S1399004714000078
48. Kuntal BK, Aparoy P, Reddanna P (2010) EasyModeller: A graphical interface to MODELLER. *BMC Res Notes* 3:226. doi: 10.1186/1756-0500-3-226
49. Pronk S, Páll S, Schulz R, et al (2013) GROMACS 4.5: a high-throughput and highly parallel open source molecular simulation toolkit. *Bioinformatics* 29:845–854. doi: 10.1093/bioinformatics/btt055
50. Berendsen HJC, Grigera JR, Straatsma TP (1987) The missing term in effective pair potentials. *J Phys Chem* 91:6269–6271. doi: 10.1021/j100308a038
51. Reif MM, Hünenberger PH (2011) Computation of methodology-independent single-ion solvation properties from molecular simulations. IV. Optimized Lennard-Jones interaction parameter sets for the alkali and halide ions in water. *J Chem Phys* 134:144104. doi: 10.1063/1.3567022
52. Brown D, Clarke JHR (1984) A comparison of constant energy, constant temperature and constant pressure ensembles in molecular dynamics simulations of atomic liquids. *Mol Phys*

51:1243–1252. doi: 10.1080/00268978400100801

53. Hess B, Bekker H, Berendsen HJC, Fraaije JGEM (1997) LINCS: A linear constraint solver for molecular simulations. *J Comput Chem* 18:1463–1472. doi: 10.1002/(SICI)1096-987X(199709)18:12<1463::AID-JCC4>3.0.CO;2-H
54. Darden T, York D, Pedersen L (1993) Particle mesh Ewald: An $N \log(N)$ method for Ewald sums in large systems. *J Chem Phys* 98:10089.
55. Humphrey W, Dalke A, Schulten K (1996) VMD - Visual Molecular Dynamics. *J Mol Graph* 14:33–38.
56. Isse AA, Gennaro A (2010) Absolute Potential of the Standard Hydrogen Electrode and the Problem of Interconversion of Potentials in Different Solvents. *J Phys Chem B* 114:7894–7899. doi: 10.1021/jp100402x
57. Mauk AG, Moore GR (1997) Control of metalloprotein redox potentials: what does site-directed mutagenesis of hemoproteins tell us? *JBIC J Biol Inorg Chem* 2:119–125. doi: 10.1007/s007750050115
58. Bortolotti CA, Siwko ME, Castellini E, et al (2011) The Reorganization Energy in Cytochrome c is Controlled by the Accessibility of the Heme to the Solvent. *J Phys Chem Lett* 2:1761–1765.
59. Moser CC, Page CC, Dutton PL (2006) Darwin at the molecular scale: selection and variance in electron tunnelling proteins including cytochrome c oxidase. *Philos Trans R Soc Lond B Biol Sci* 361:1295–1305. doi: 10.1098/rstb.2006.1868
60. Khoshtariya DE, Dolidze TD, Shushanyan M, Davis KL (2010) Fundamental signatures of short- and long-range electron transfer for the blue copper protein azurin at Au / SAM junctions. *Proc Natl Acad Sci USA* 107:2757–2762. doi: 10.1073/pnas.0910837107
61. Gray HB, Malmström BG, Williams RJP (2000) Copper coordination in blue proteins. *J Biol Inorg Chem* 5:551–559. doi: 10.1007/s007750000146
62. Milischuk AA, Matyushov D V., Newton MD (2006) Activation entropy of electron transfer

- reactions. *Chem Phys* 324:172–194. doi: 10.1016/j.chemphys.2005.11.037
63. Farver O, Marshall NM, Wherland S, et al (2013) Designed azurins show lower reorganization free energies for intraprotein electron transfer. *Proc Natl Acad Sci U S A* 110:10536–40. doi: 10.1073/pnas.1215081110
 64. Iwaki M, Itoh S (1989) Electron transfer in spinach photosystem I reaction center containing benzo-, naphtho- and anthraquinones in place of phyloquinone. *FEBS Lett* 256:11–16. doi: 10.1016/0014-5793(89)81708-9
 65. Moser CC, Farid T a, Chobot SE, Dutton PL (2006) Electron tunneling chains of mitochondria. *Biochim Biophys Acta* 1757:1096–109. doi: 10.1016/j.bbabo.2006.04.015
 66. Gray HB, Winkler JR (1996) Electron Transfer in Proteins. *Annu Rev Biochem* 65:537–561.
 67. Murgida DH, Hildebrandt P (2002) Electrostatic-Field Dependent Activation Energies Modulate Electron Transfer of Cytochrome c. *J Phys ChemB* 106:12814–12819.
 68. Corni S (2005) The reorganization energy of azurin in bulk solution and in the electrochemical scanning tunneling microscopy setup. *J Phys Chem B* 109:3423–30. doi: 10.1021/jp0459920
 69. Daidone I, Amadei A (2012) Essential dynamics: foundation and applications. *Wiley Interdiscip Rev Comput Mol Sci* 2:762–770. doi: 10.1002/wcms.1099
 70. Kiger L, Tilleman L, Geuens E, et al (2011) Electron transfer function versus oxygen delivery: A comparative study for several hexacoordinated globins across the animal kingdom. *PLoS One*. doi: 10.1371/journal.pone.0020478
 71. Weiland TR, Kundu S, Trent JT, et al (2004) Bis-histidyl hexacoordination in hemoglobins facilitates heme reduction kinetics. *J Am Chem Soc* 126:11930–11935. doi: 10.1021/ja046990w
 72. De Sanctis D, Pesce A, Nardini M, et al (2004) Structure-function relationships in the growing hexa-coordinate hemoglobin sub-family. *IUBMB Life* 56:643–651. doi: 10.1080/15216540500059640

73. Wilson MT, Greenwood C, Brunori M, Antonini E (1975) Kinetic studies on the reaction between cytochrome c oxidase and ferrocytochrome c. *Biochem J* 147:145–153.
74. Guidolin D, Agnati LF, Tortorella C, et al (2014) Neuroglobin as a regulator of mitochondrial-dependent apoptosis: A bioinformatics analysis. *Int J Mol Med* 33:111–116. doi: 10.3892/ijmm.2013.1564
75. Kakar S, Hoffman FG, Storz JF, et al (2010) Structure and reactivity of hexacoordinate hemoglobins. *Biophys Chem* 152:1–14. doi: 10.1016/j.bpc.2010.08.008
76. Huberts DHEW, van der Klei IJ (2010) Moonlighting proteins: An intriguing mode of multitasking. *Biochim Biophys Acta - Mol Cell Res* 1803:520–525. doi: <http://dx.doi.org/10.1016/j.bbamcr.2010.01.022>
77. Jeffery CJ (2015) Why study moonlighting proteins? *Front Genet* 6:211. doi: 10.3389/fgene.2015.00211